Biophysical Chemistry 20 (1984) 39–59
Elsevier

BPC 00863

CURRENT-VOLTAGE CHARACTERISTICS AND SELF-SUSTAINED OSCILLATIONS IN DIOLEYL PHOSPHATE-MILLIPORE MEMBRANES

Kiyoshi TOKO, Masaru TSUKIJI, Shu EZAKI * and Kaoru YAMAFUJI

Department of Electronics, Faculty of Engineering, Kyushu University 36, Fukuoka 812, Japan

Received 2nd December 1983
Revised manuscript received 30th January 1984
Accepted 1st February 1984

Key words: Phase transition; I-V characteristics; Self-oscillation; Burst; Model membrane

For an artificial membrane prepared by infiltrating dioleyl phosphate (DOPH) into pores of a Millipore filter, we propose a theoretical model for explaining observed data on electric behavior, such as d.c. current-voltage characteristics and self-sustained oscillations of the electric potential. The model consists of a simple electric circuit composed of electric resistances and capacitances as given functions of internal variables which represent conformational states of DOPH molecules and salt concentration inside the pore concerned. The kinetic equations for these variables are the same as those presented previously for describing a phase transition of DOPH, except for a slight modification taking account of effects of salt accumulation inside the pore. The present theory can describe well the I-V hysteresis and various features of spike-like oscillations with long periods of up to a few hours in the absence of external force and also short-period oscillations with periods of the order of 1 s under pressure difference.

1. Introduction

A DOPH-Millipore membrane is composed of a Millipore filter whose pores are choked up with a lipid analogue, dioleyl phosphate (DOPH). This model membrane displays an appreciable variation in electric capacitance, electric resistance or membrane potential near the critical concentration n_t of salt, such as KCl. These phenomena are attributed to a phase transition of DOPH molecules in pores, where the transition occurs between hydrophobic oil droplets at lower salt concentrations and hydrophilic micelles or bilayer (or sometimes multilayer) leaflets at higher concentrations [1–3].

Two kinds of self-sustained oscillations of electric potential V with quite different periods have also been found, according to the experimental conditions. One is the self-oscillation with a rather long period between several minutes and a few hours, which appears in the absence of applied forces such as electric current I_a, electric voltage difference V_a and pressure difference ΔP_a [4]. The other has a short period of the order of 1 s observed only in the presence of some imposed external forces [5,6]. Several theories have been presented to account for these self-sustained oscillations [6,7]. However, these theories are not sufficient for describing detailed characteristics such as their wave forms, apart from the fact that each kind of oscillation has been explained by means of each of the models, which are different from one another.

The d.c. current-voltage relation of the DOPH-Millipore membrane is known to be quite characteristic owing to the appearance of a hysteresis curve of the observed electric current I with variation in V_a as well as a hysteresis curve of the observed electric voltage V under control of I_a [2,6]. While such a current-voltage relation may

* Present address: Toshiba Corporation (Nasu Works) 1385-1, Shimoishigami, Otawara, Tochigi 329-26, Japan.

result from the phase transition of DOPH molecules in pores, no quantitative explanation of the relation has been provided so far.

The purpose of this paper is to discuss comprehensively long- and short-period oscillations as well as the d.c. current-voltage characteristics in a DOPH-Millipore membrane, based on a single theoretical model. The present model consists of an equivalent electric circuit model of the system composed of electric capacitances and electric resistances which reflect the conformational states of DOPH molecules in the relevant pore. As mentioned later in detail, only one pore is considered to participate in oscillations. The kinetic equations for describing the conformational change in DOPH molecules in the pore are formally the same as those presented previously [3,7]. However, the effect of salt accumulation in the pore is taken into account in the present theory to explain the large degree of difference in the duration between long- and short-period oscillations: In the presence of an applied pressure ΔP_a, the resultant salt accumulation above the critical salt concentration n_t in a pore forces the majority of DOPH molecules to undergo slow phase transitions to multilayers. Since only an extremely small proportion of the total number of DOPH molecules in the pore concerned at the side of lower external salt concentration has a chance of encountering salt concentrations lower and higher than n_t according to the conformational states of DOPH, it repeats phase transitions rapidly to result in short-period oscillations. In the absence of an external pressure difference, on the other hand, the salt concentration in the pore may be relatively low due to little penetration of salt under the concentration gradient alone, which yields a long-period oscillation accompanied by a slow repeat of phase transitions of a large fraction of DOPH molecules in the pore.

Since the electric behavior of DOPH-Millipore membranes is known to be quite sensitive to the preparation conditions of samples, a series of experimental results observed in the samples for which details of the preparation conditions are known well is clearly better for quantitative comparison with theoretical results. Some of the experimental results obtained in this manner are summarized in section 2, together with the behavior of a bursting-like oscillation containing successive wave bundles composed of oscillations with a period of several seconds. The present theoretical model is introduced in section 3 as a set of general equations. A reduction of the general equations so as to be applicable to each observed phenomenon is carried out in section 4. In section 5, these theoretical results are quantitatively compared with the experimental results described in section 2.

2. Experimental results

The DOPH-Millipore membranes used in the present experiments were prepared by the same method as reported previously [7]. Millipore filter papers of 8 μm pore size were used, and the membranes were immersed in 5 mM KCl solution so that DOPH molecules were expected to be oil droplets before measurements. Each membrane was placed between two cells with two pairs of Ag-AgCl electrodes, one of which was used for the measurement of membrane potential or voltage difference across the membrane, the other being for the current supply. In the case of voltage supply, the current was estimated from the induced voltage difference at both ends of a 20 kΩ resistance. The cells were manufactured so that the pressure difference ΔP_a could be imposed on the membrane.

Fig. 1 shows an example of self-oscillations with a period of about 30 min when the membrane was placed between 5 and 100 mM KCl solutions. This type of oscillation usually began several hours after the membrane had been placed between the two cells, which implies that it takes several hours until salt has penetrated deeply into pores to induce slow phase transitions of DOPH [3]. In spite of the long period of about 30 min, the wave form is spike-like with a pulse width of only about 4 min, as has been reported to be a noticeable feature in long-period oscillations [2,7]. The period increased with increase in the amount of DOPH adsorbed in the filter (Q), the pulse width also increasing to a small extent [7]. When the electric current I_a was imposed on the membrane, the period decreased gradually for increasing I_a, the oscillation finally stopping for $I_a = 0.4$ μA [7].

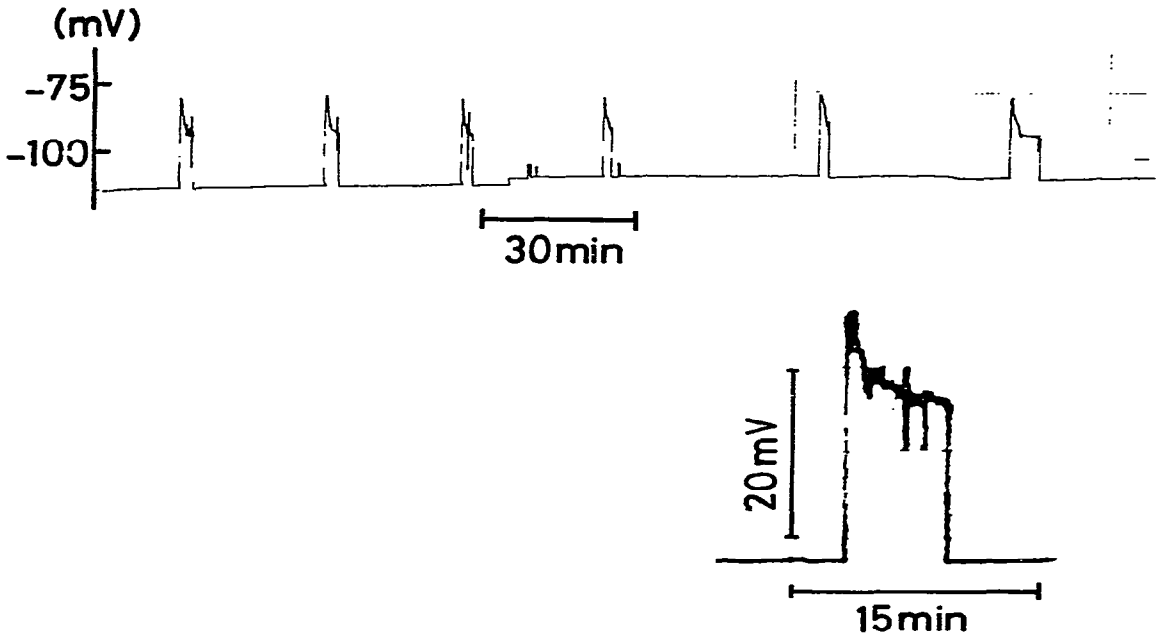

Fig. 1. An example of long-period oscillations with $Q = 5.6$ mg/cm^2. The electric voltage difference was measured at the origin of the cell on the 5 mM side.

Fig. 2 shows an example of self-oscillations with a period of about 1 s observed when a pressure difference of 33 cmH_2O and a current of 0.6 μA were imposed on the membrane from the 100 mM to 5 mM side. Whereas the occurrence of such short-period oscillations does not always require the current supply [5], application of the current usually makes self-oscillations begin soon after the pressure difference has been imposed, and hence all experiments on this type of oscillation usually finish before the long-period oscillation begins. An increase in the pressure difference ΔP_a above some threshold value ΔP_{th} brings about an oscillatory state of the membrane [5,6]. Even below the threshold value ΔP_{th}, however, the oscillation appears for an increase in current I_a above some threshold value I_{th} [6]. The frequency of oscillation increases almost linearly for further increase in ΔP_a or I_a. It is noticeable that the imposed current I_a stops long-period oscillations, while I_a brings about short-period oscillations.

Fig. 3 shows an example of bursting-like oscilla-

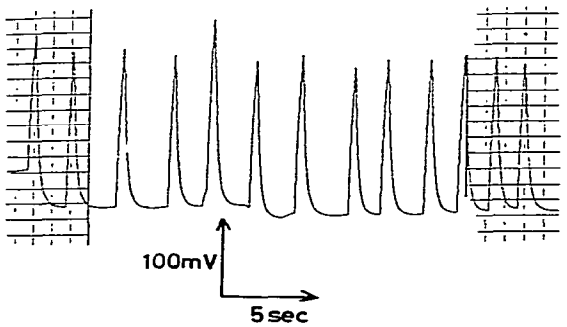

Fig. 2. An example of short-period oscillations with $Q = 3.6$ mg/cm^2 under $\Delta n_a = 95$ mM, $\Delta P_a = 33$ cmH_2O and $I_a = 0.6$ μA.

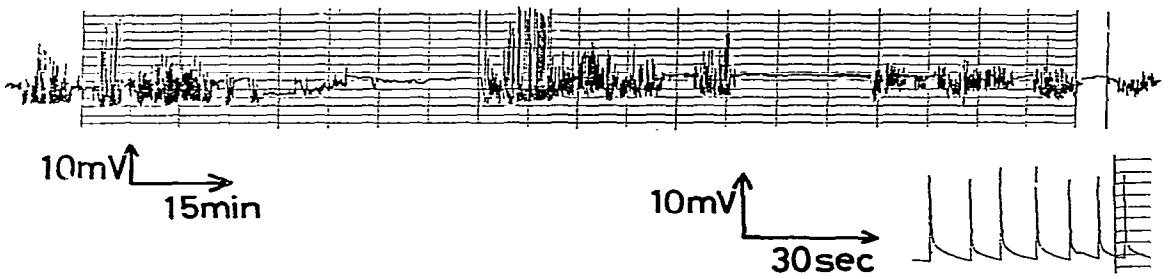

Fig. 3. An example of bursting-like oscillations with $Q = 3.1$ mg/cm^2 when the membrane was placed between 5 mM and 100 mM KCl solutions.

tions which sometimes appear even under no imposed external force such as ΔP_a or I_a. It should be noted that this type of oscillation appears several hours after the gradient of salt concentration has been imposed, instead of long-period oscillations. In fact, the period between successive bursting bundles is of the order of 1 h. As shown in the inset to fig. 3, however, the period and wave form of each wave in the bundle closely resemble those in the short-period oscillations under ΔP_a and I_a shown in fig. 2. This suggests that the mechanism of short-period oscillations does not differ greatly from that of long-period oscillations, although the presence of a pressure difference may affect the

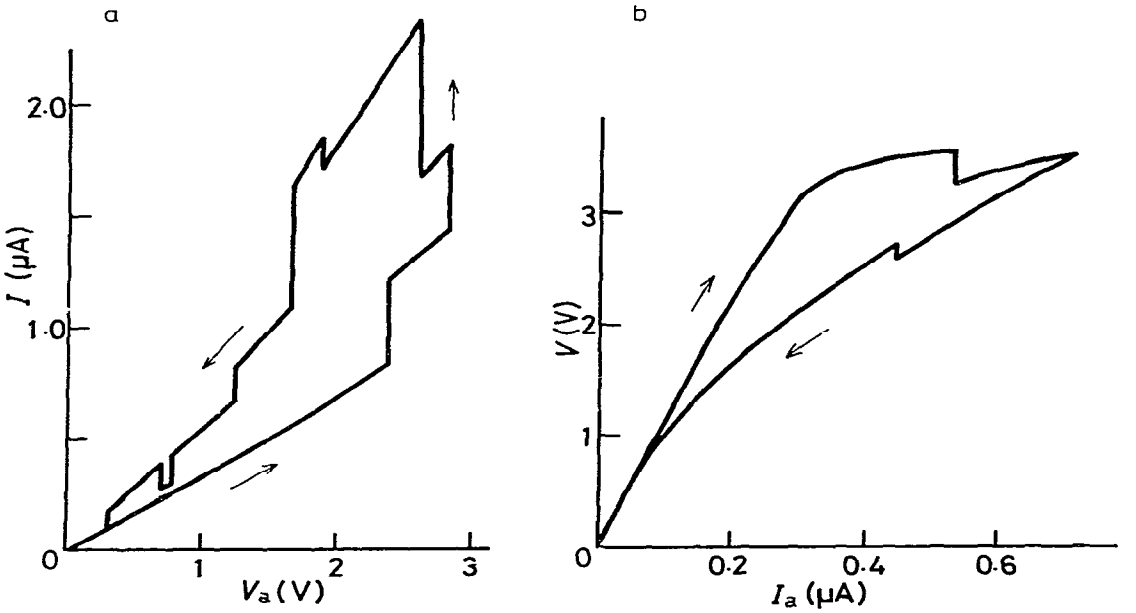

Fig. 4. Examples of d.c. current-voltage characteristics. (a) The lower and higher salt concentrations in two cells were chosen as 5 and 100 mM, respectively. The pressure difference of 52 cmH_2O was imposed on the membrane with $Q = 3.6$ mg/cm^2. (b) The salt concentrations were equal to 5 mM, and ΔP_a was not imposed. $Q = 4.8$ mg/cm^2.

value of average salt concentration and accordingly the conformational states of DOPH molecules in pores. Such peculiar oscillations probably appear only when DOPH molecules are adsorbed tightly so that their distribution is probably nonuniform inside the pore concerned and also near the surfaces of the filter.

Fig. 4 illustrates typical examples of the d.c. current-voltage characteristics with hysteresis curves, where many spikes appearing randomly [4] are omitted. These characteristics can be obtained irrespective of the presence or absence of an external pressure difference and/or salt-concentration difference across the membrane, provided the salt concentration at least in one cell is lower than the critical concentration n_t ($= 30$ mM).

3. A theoretical model

In this section, let us first present a set of kinetic equations for the phase transition of DOPH and salt concentration, which can be used even in the presence of external salt-concentration difference Δn_a, pressure difference ΔP_a and electric current I_a. Next, an equivalent electric-circuit model is introduced to connect the internal variables appearing in the kinetic equations for DOPH with the observable quantity such as I or V.

3.1. Equations for length of the phase-transition region, DOPH molecules and salt concentration

3.1.1. Length of the phase-transition region inside a pore

According to Kobatake's [1,2] suggestions and some related experimental facts [8], DOPH molecules are considered to undergo transitions between three phases composed of oil droplets, spherical micelles and multilayers. If the external salt concentrations in the right and left cells are equal, the phase transition can be discussed by regarding both the conformational states of DOPH and the salt concentration as macroscopically homogeneous along the pore wall [3].

If the salt concentration in one cell is different from that in the other, however, the situation becomes more complex. DOPH molecules in only one pore may repeat phase transitions and hence are responsible for the observed self-oscillations, as described quantitatively in section 3.2 and the Appendix. The salt concentration inside a pore is supposed to increase gradually from the side of the cell with a lower salt concentration, n_l, to the opposite side with a higher concentration, n_h. By considering first a stationary state of the salt concentration inside the pore, we obtain the macroscopic features of internal variables such as the salt concentration and the conformational states of DOPH. This enables us to estimate the size of the region where DOPH molecules participate in self-oscillations. To discuss self-oscillations, it is sufficient to focus on describing the kinetic behavior of DOPH and salt concentration only within this region.

Fig. 5 illustrates the conformational states of DOPH in a pore under Δn_a ($= n_h - n_l > 0$), ΔP_a and I_a, where a DOPH molecule is illustrated as a small circle with two 'tails'. DOPH molecules may make an assembly form of hydrophobic oil droplets at lower salt concentrations but hydrophilic micelles or multilayers at higher salt concentrations [1–3]. Oil droplets can be considered as large aggregates composed of many loosely packed lipids in a random phase, which are shown schematically by the amorphous shapes occupied by dots in fig. 5. Spherical micelles are, on the other hand, formed from about 100 lipids, and multilayers have planar lamellar structures with tight packing, while all polar head groups are in contact with the aqueous phase. The fact that DOPH can form black membranes in a relatively concentrated solution [1,2] may suggest that DOPH filling pores of the Millipore filter can also form bilayers or multilayers in consideration of the observation for phosphatidylcholines of multilayer formation in filter pores [8]. A direct transformation, however, from oil droplets to bilayers or multilayers is not expected to occur so easily under the usual conditions because of the large size of the oil droplets. In the model, therefore, oil droplets are supposed as having been transformed to many small micelles in the first stage of increasing salt concentration. Thereafter, some of them diffuse into an equilibration layer, inside which they can undergo electric and van der Waals interactions with multilayers.

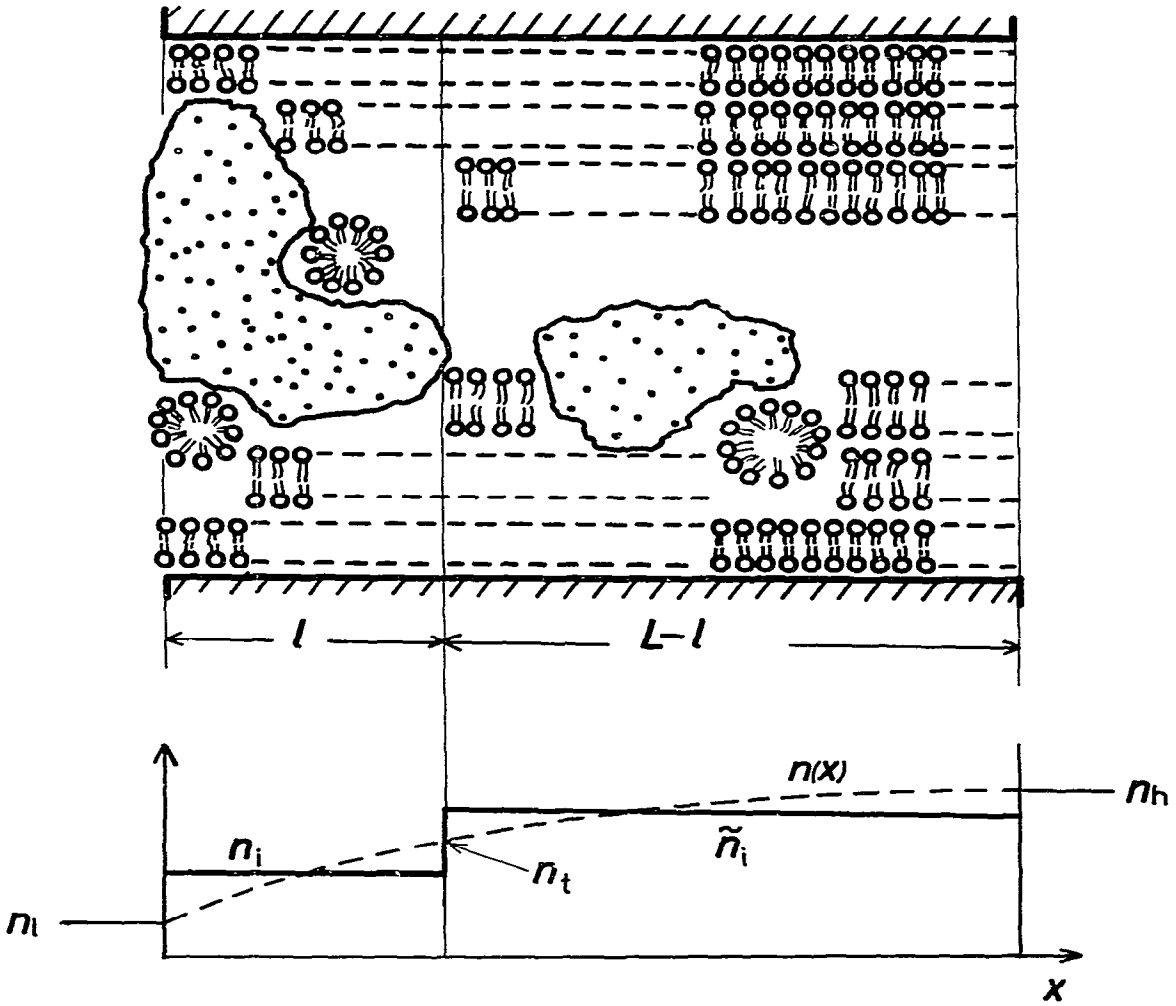

Fig. 5. Illustration of conformations of DOPH molecules and salt concentration within a pore under Δn_a, ΔP_a and I_a. The dashed line in the lower figure shows $n(x)$ given by eq. 3, and the solid line denotes n_i and $\tilde{n}_i$ in the phase-transition and higher salt-concentration regions, respectively.

being incorporated into multilayers [3], as expressed explicitly later.

In fig. 5, the major fraction of DOPH is composed of oil droplets in the region of salt concentration lower than the critical concentration n_t and multilayers in the region of salt concentration higher than n_t. The local salt concentration inside a pore may change almost monotonically from n_l to n_h along the pore wall arrayed almost perpendicular to the filter surface. As has been pointed

out [7], however, the repetition of phase transitions among three phases of DOPH molecules mainly occurs in the region of lower salt concentration, where the accumulation and release of salt occurs accompanied by repeating phase transitions. The region of higher salt concentration occupied mainly by the multilayer phase does not contribute to the oscillations, owing to the impossibility of a transformation from multilayers to oil droplets [7]. Even if the majority of DOPH molecules remain in the oil-droplet phase for several hours after the membrane has been placed between two cells, they cannot repeat phase transitions among three phases due to the presence of high salt concentration, but tend to change slowly to multilayers.

Thus, we divide the region inside the pore into two regions in order to simplify the problem by reducing it to a zero-dimensional one [9]. In other words, we shall adopt the approximation that the salt concentration is spatially constant in each region, as shown in fig. 5, where the salt concentrations in the regions of lower and higher salt concentrations are denoted by n_i and $\bar{n}_i$, respectively. Since the region of lower salt concentration directly relates to oscillations originating from the repeating phase transitions of DOPH, we here term this region a phase-transition region.

The length of the phase-transition region, l, may be defined so that the stationary concentration in this region is lower than the critical concentration n_t (= 30 mM), above which the major fraction of DOPH is transformed into multilayers. For the purpose of deriving an expression for l as a function of Δn_a, ΔP_a and I_a (or V_a), let us use the phenomenological equations for the salt concentration $n(x)$ which have been adopted in a glass-filter system [10]:

$$\begin{aligned} U_m &= -A\frac{\partial P}{\partial x} - B\frac{\partial \phi}{\partial x}, \\ i &= -\Lambda n\frac{\partial \phi}{\partial x} - \Lambda'\frac{\partial n}{\partial x}, \\ J_s &= -D\frac{\partial n}{\partial x} + D' n\frac{\partial \phi}{\partial x} + nU_m, \end{aligned} \tag{1}$$

where U_m is the mass flow, i the electric current and J_s denotes the salt flow within the relevant pore. The pressure, electric potential and salt concentration within the pore along the x-axis are designated by P, ϕ and n, respectively. The relevant phenomenological coefficients are introduced by A, B, Λ, Λ', D and D'.

Eq. 1 has a constant numerical coefficient, B, while the corresponding coefficient is $B/\sqrt{n}$ in the glass-filter system [10] due to the presence of fixed charge. The dynamic conformational change in DOPH molecules has been suggested to play an essential role in phenomena such as variations in electric characteristics with changing salt concentration and self-sustained oscillations of membrane potential [1–7]. We omitted the $\sqrt{n}$ dependence for simplicity and performed linearization in the expression for U_m, since this dependence no longer seems to hold in such a complex system as that considered here and rather a nonlinearity expressed by the phase transition of DOPH may be indispensable to an explanation of the observed experimental facts in this system.

Let us assume a stationary state given by

$$\mathrm{div} U_m = \mathrm{div} i = \mathrm{div} J_s = 0. \tag{2}$$

Taking into account the boundary conditions of $n = n_l$ at $x = 0$ and $n = n_h$ at $x = L$, we obtain the expression for $n(x)$:

$$n(x) = \frac{1}{1 - \exp\left(\frac{U_m L}{\tilde{D}}\right)}\left[n_h - n_l \exp\left(\frac{U_m L}{\tilde{D}}\right) - \Delta n_a \exp\left(\frac{U_m x}{\tilde{D}}\right)\right], \tag{3}$$

where $\tilde{D}$ is given by

$$\tilde{D} = D + D'\frac{\Lambda'}{\Lambda}. \tag{4}$$

It may be more convenient to express U_m in terms of the applied pressure difference ΔP_a and the electric voltage difference V by means of the relevant phenomenological positive coefficients L_p and L_v, respectively, as follows:

$$U_m = -L_p \Delta P_a - L_v V. \tag{5}$$

The length of the phase-transition region, l, can be estimated by putting $n(l) = n_t$ from the definition, and is given by

$$l = L + \frac{\tilde{D}}{U_m} \ln\left[\left(1 - \frac{\Delta n_t}{\Delta n_a}\right) \exp\left(-\frac{U_m L}{\tilde{D}}\right) + \frac{\Delta n_t}{\Delta n_a}\right] \tag{6}$$

with Δn_t given by

$$\Delta n_t = n_t - n_i. \tag{7}$$

As can be seen from eqs. 5 and 6, the length l decreases for increasing ΔP_a or V.

The values of numerical parameters such as L_p and L_s are summarized in table 1 in the appendix together with the other parameters.

If the external salt concentrations in two cells are equal, we set $\Delta n_t/\Delta n_a$ in eq. 6 as equal to unity, which leads to $l = L$ as expected.

3.1.2. Kinetic equations for the phase transition of DOPH molecules

The equations for the phase transition of DOPH molecules are the same as those in the previous papers [3,7]. If we define η, η_m and η_s as the fractions of DOPH molecules in micelles in the inner bulk layer far from the pore wall, multilayers near and parallel to the wall and micelles in the equilibration layer in contact with each phase, respectively, kinetic equations for DOPH may be given by

$$\frac{d\eta}{dt} = k_1(1 - \eta - \eta_s - \eta_m)n_i - k_{-1}\eta + k_{-D}\eta_s - k_D\eta. \tag{8a}$$

$$\frac{d\eta_s}{dt} = -k_{-D}\eta_s + k_D\eta + k_{-2}\eta_m - k_2\eta_s. \tag{8b}$$

$$\frac{d\eta_m}{dt} = -k_{-2}\eta_m + k_2\eta_s. \tag{8c}$$

where the coefficients k_1, k_{-1}, k_2, k_{-2}, k_D and k_{-D} designate the relevant rate constants. The fraction of DOPH in oil droplets corresponds to $(1 - \eta - \eta_s - \eta_m)$. The salt concentration n_i refers to that in the phase-transition region with length l, which approaches the length L of the whole region in a pore when the external salt-concentration difference Δn_a is decreased.

Among the rate constants, k_D and k_{-D} reflect the well-known relation between a diffusion constant and a free volume [11]:

$$k_D = v^{-1}k_{-D} = D_0 \exp\left[-d_1/(1 + d_2\eta_m^2)\right]. \tag{9}$$

where v designates the volume ratio of the equilibration layer to the inner one, and D_0, d_1 and d_2 are numerical parameters. DOPH molecules in the solution inside the pore can move more easily as the free volume is increased accompanied by development of the multilayer phase.

An expression for the rate constant k_{-2} was derived by taking account of an electrochemical free energy of the system composed of the charged multilayer and aqueous solution [12,13]:

$$k_{-2} = k^0_{-2}/n_i, \tag{10}$$

with the constant k^0_{-2}.

Eqs. 8a–c can be reduced to more simplified ones, if we note that the values of k_D and k_{-D} are much smaller than those of other rate constants. With the aid of a quasi-stationary approximation, we obtain [7]

$$\frac{d\zeta}{dt} = k_1(1 - \zeta - \eta_m)n_i - k_{-1}\left[\zeta - (k_{-2}/k_2)\eta_m\right]. \tag{11a}$$

$$\frac{d\eta_m}{dt} = k_D\left[(k_2/k_{-2})\zeta - (1 + v)\eta_m\right], \tag{11b}$$

where ζ is the total fraction of spherical micelles defined by

$$\zeta = \eta_s + \eta. \tag{12}$$

In this paper, we shall take into account explicitly the effects of Δn_a, ΔP_a and I_a on these equations to describe self-oscillations and the d.c. current-voltage characteristics. In the present theory these effects are expressed through the dependences of l given by eq. 6 on Δn_a, ΔP_a and I_a. Since eqs. 8 and 11 represent overall reactions of DOPH molecules in pores, the rate constants should depend on the number of DOPH molecules related directly to the phase transition contributing to self-oscillations, and the values of such rate constants are known to increase as the number of molecules involved decreases [14]. As mentioned above, DOPH molecules responsible for oscillations belong to the region of lower salt concentration shown in fig. 5, i.e., the phase-transition region. Since the number of molecules concerned may decrease while length l decreases in the present model, the rate constants are considered to

increase as functions of l. Thus, we assume the following simple relation between them, because a detailed selection of functional forms scarcely alters the final results:

$$k_1 = k_1^*/(l/L),\ D_0 = D_0^*/(l/L), \tag{13}$$

and so on.

Eqs. 8 and 11 with the rate constants of eqs. 9, 10 and 13 through eq. 6 are the basic equations to describe the kinetics of phase transitions of DOPH even in the presence of Δn_a and ΔP_a, if the salt concentration n_i is given explicitly. As will be seen later, oscillations occur as a result of phase transitions of DOPH coupled with kinetics of salt concentration.

3.1.3. Equation for the salt concentration n_i

In this section we deal with a kinetic equation for the salt concentration n_i, which is the average quantity in the phase-transition region (or the whole region in a pore when the salt-concentration difference is not imposed). When the salt concentrations n_o in two cells are equal, n_i is considered as nearly equal to n_o for small adsorbed amounts of DOPH, which is really the case performed in usual experiments [1–3].

If the salt-concentration difference Δn_a is imposed across the Millipore membrane, n_i becomes dependent on the conformational states of DOPH, as already pointed out [7]: if the greater part of the DOPH molecules form multilayers, n_i may be reduced to nearly n_l, since this phase may be packed compactly to result in empty space in the pore, which adjoins the phase-transition region to the left cell with n_l in fig. 5. In fact, DOPH molecules in higher salt concentrations show lower electric resistance [1,2]. If micelle and oil-droplet phases develop as a result of depletion of the multilayer phase, n_i may increase almost to n_h, because the phase-transition region and the left cell break off as a result of the interruption through hydrophobic oil droplets and salt is accumulated in the hydrophilic micelle phase by the penetration from the side of right cell with n_h.

Furthermore, we must take into account an effect of the imposed current I_a or voltage V_a on n_i. This effect will be described in detail later when discussing the electric circuit model. Owing to the existence of a large electric capacitance of $(10^4–3\times10^5)$ pF/cm^2, the DOPH-Millipore membrane behaves as a kind of electric capacitor.

In the zero-dimensional approach [9], the equation for n_i can be written as

$$\frac{dn_i}{dt} = \hat{D}[\hat{n} - n_i], \tag{14}$$

with $\hat{n}$ defined by

$$\hat{n} = X_N[X_A + (1 - X_A)\hat{f}_1(\zeta)] \times [1 - (1 - X_B)\hat{f}_2(\eta_m)] + \hat{n}_a, \tag{15}$$

where X_N, X_A and X_B are the numerical parameters, and the final term $\hat{n}_a$ expresses salt accumulated due to the applied current I_a or voltage V_a, as given later explicitly in the electric circuit model. The functions $\hat{f}_1$, $\hat{f}_2$ and $\hat{D}$ may be given by [7]

$$\hat{f}_1(\zeta) = (\zeta/\zeta_c)^\gamma\left[1 + (\zeta/\zeta_c)^\gamma\right]^{-1}, \tag{16a}$$

$$\hat{f}_2(\eta_m) = (\eta_m/\eta_{mc})^{\gamma'}\left[1 + (\eta_m/\eta_{mc})^{\gamma'}\right]^{-1}, \tag{16b}$$

$$\hat{D} = \hat{D}_0 \exp\left\{-\hat{d}_1/\left[1 + \hat{d}_2(\zeta + \eta_m)^2\right]\right\}. \tag{17}$$

In eqs. 16a and b, the numerical constants are γ, γ', ζ_c and η_{mc}. The functions $\hat{f}_1$ and $\hat{f}_2$ are constructed in order to express the above-mentioned features that the multilayer phase releases salt while the spherical-micelle phase accumulates salt. In eq. 17, diffusion of salt is expressed in almost the same way as that of DOPH given in eq. 9. The smaller the amount of oil droplets, the faster the salt may move in the pore. The numerical parameters included in the diffusion coefficient $\hat{D}$ are designated by $\hat{d}_1$ and $\hat{d}_2$, and the parameter for expressing the magnitude of diffusion speed, $\hat{D}_0$, may depend on the amount of DOPH adsorbed and the volume of the region concerned as already pointed out [7]. When the equation for n_i is expressed by eq. 14, it is reasonable to assume $\hat{D}_0$ as being inversely proportional to the square of (l/L):

$$\hat{D}_0 = \hat{D}_0^*/(l/L)^2, \tag{18}$$

with the numerical constant $\hat{D}_0^*$.

3.2. Equivalent electric-circuit model

Fig. 6 shows a description of the system by means of electric resistances and capacitances, where the situation of equal salt concentrations in two cells is depicted in panel a, and the case with Δn_a, ΔP_a and I_a for oscillations is in panel b. It can be easily seen that fig. 6a corresponds to the limiting case of fig. 6b at $\Delta n_a = 0$.

Let us first discuss fig. 6a. Since the electric resistance R_T and the electric capacitance C_T of the membrane are much larger than those in the aqueous solution, the measured values of electric characteristics are considered to be reflected by R_T and C_T to a good approximation at the applied frequency of 1 kHz used previously [3], where drastic changes in electric characteristics are observed [1]. In fact, a fairly good agreement between the theoretical result of C_T and the observed data was obtained, if C_T was assumed as being proportional to the fraction of multilayers η_m with the numerical coefficient C_T^0:

$$C_T = C_T^0 \eta_m. \tag{19a}$$

Thus, it may be reasonable to adopt this relation for C_T.

The electric resistance R_T, on the other hand, may be related to internal variables such as the salt concentration n_i and the conformational states of DOPH. Let us express R_T in the following form so as to reproduce the observed transition-like change near n_t:

$$R_T(n_i) = \frac{r_l + r_h \exp[\hat{\gamma}(n_i - n_t)]}{1 + \exp[\hat{\gamma}(n_i - n_t)]}, \tag{19b}$$

with

$$r_h = \frac{r_h^0}{n_i}, \tag{20}$$

where r_l, r_h^0 and $\hat{\gamma}$ are the numerical parameters, and the subscripts l and h denote lower and higher salt concentrations, respectively. Eq. 19b is reduced to r_l of several megohms at lower concentrations and r_h given by eq. 20 at higher concentrations, which is inversely proportional to n_i ($= n_o$ in this case), as observed [1,2].

We next discuss the case depicted in fig. 6b, where oscillations occur under Δn_a. While about 10^6 pores per unit area (cm^2) are contained in a filter, only one pore is considered to be involved in oscillations. As mentioned in the appendix, our estimate of electric resistance supports the possibility of one pore being concerned with oscillations. While oscillations probably originating from two pores sometimes appeared, they usually could not continue, as also shown in fig. 12. In addition, the amount of DOPH adsorbed is necessarily large

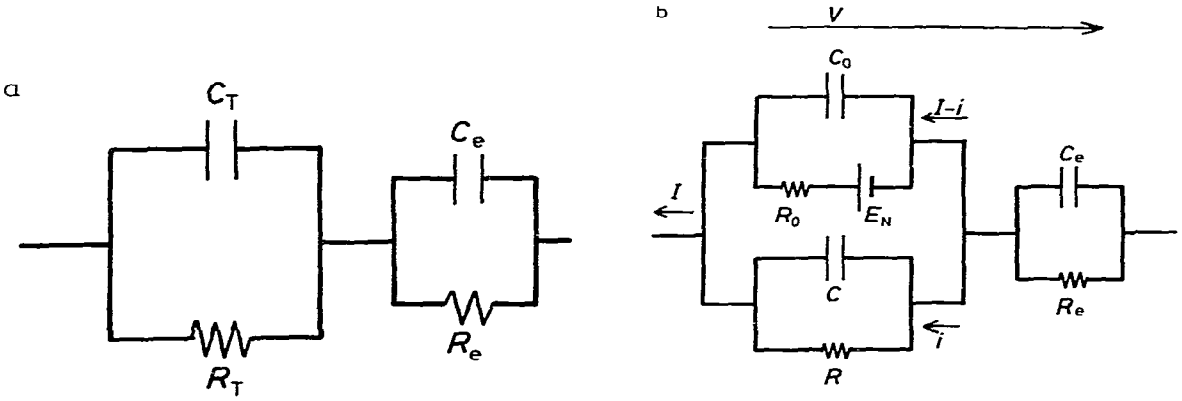

Fig. 6. Equivalent electric-circuit model. The electric quantities in the external aqueous solutions are denoted by C_e and R_e. The electric characteristics of the DOPH-Millipore membrane are expressed by the electric circuit composed of C_T and R_T in panel a or that of C_0, R_0, C, R and E_N in panel b. A limiting case of b when Δn_a is zero corresponds to a.

for the occurrence of oscillation [7]. It would take too much time for all DOPH molecules to make transitions. In this situation, self-oscillations are supposed to appear in some pore containing the small adsorbed amount compared with those in other pores. As shown later, the calculated results of oscillations based on the above idea in practice give a good agreement with observed data.

The electric circuit of a membrane consists of two parallel parts, one of which represents an open pore occupied by DOPH molecules responsible for self-oscillations, the other representing the remaining closed pores choked up by DOPH molecules of oil droplets. While the former is expressed by the parallel circuit of R and C in fig. 6b, the latter is expressed by C_0 with parallel elements of R_0 and the e.m.f. E_N. While the e.m.f. is not shown in the pore related to oscillations, it may be considered as equal to a diffusion potential, which has a value of nearly zero for KCl, due to sufficient penetration of salt into the pore concerned probably with relatively small amounts of adsorbed DOPH.

These elements are intimately related to the conformational states of DOPH as well as the salt concentration. Among them, however, such elements in closed pores as R_0 and C_0 contributing in no direct way to oscillations are regarded as constant. The e.m.f. E_N is now considered as the Nernst potential:

$$E_N = 59.2 \log\left(\frac{n_h}{n_l}\right), \tag{21}$$

where the numerical coefficient is evaluated at 25 °C in millivolts.

As for the elements in open pores, it is reasonable to adopt almost the same relations as those expressed by eqs. 19a and b. Since the open pore, composed of two regions, lies in parallel with the remaining closed pores, the electric capacitance C is given by

$$\frac{1}{C} = \frac{N}{C_T^0}\left(\frac{l/L}{\eta_m} + \frac{1 - l/L}{\tilde{\eta}_m}\right), \tag{22a}$$

where N is roughly supposed as equal to or smaller than the number of pores, and η_m and $\tilde{\eta}_m$ designate the fractions of multilayers in the phase-transition region and the region of higher salt concentration in the open pore, respectively. The kinetics of fraction η_m is given by eq. 8c or 11b. Fraction $\tilde{\eta}_m$, on the other hand, may not change with time as much as η_m during self-oscillations, since the salt concentration is always high in this region. We therefore consider $\tilde{\eta}_m$ as approximately constant during self-oscillations. While the value of $\tilde{\eta}_m$ may be nearly zero for a few hours after the membrane has been placed between two cells, $\tilde{\eta}_m$ may approach unity after enough time has passed. This point is important for clarifying the apparent contrasting effects of the imposed current on short- and long-period oscillations, and is discussed in detail in section 6.

The electric resistance leads to

$$R(n_i, \tilde{n}_i) = N\left[R_T(n_i)\frac{l}{L} + R_T(\tilde{n}_i)\left(1 - \frac{l}{L}\right)\right], \tag{22b}$$

where $R_T(n_i)$ and $R_T(\tilde{n}_i)$ are given by eq. 19b with n_i and $\tilde{n}_i$ the salt concentrations in the relevant regions, shown in fig. 5. The salt concentration $\tilde{n}_i$ in the region of higher salt concentration may have the following form within the present scheme of approximation in fig. 5:

$$\tilde{n}_i = n_i + n_t - n_l. \tag{23}$$

Using the present equivalent electric circuit, we can easily obtain such a measured quantity as V in terms of η_m, $\tilde{\eta}_m$, n_i, $\tilde{n}_i$, n_l, n_h and I_a:

$$V = -\frac{R}{R + R_0}E_N + \frac{RR_0}{R + R_0}I_a, \tag{24a}$$

where E_N and R are given by eqs. 21 and 22b, respectively. In deriving eq. 24a, the electric resistance in the aqueous solution was omitted because of its small value compared with R_0 and R. In the open pore, the following relation holds:

$$V = Ri, \tag{24b}$$

where i is the current flowing through the open pore.

Furthermore, the voltage V is proportional to the electric charge q accumulated in the capacitance C:

$$q = CV, \tag{25}$$

with C being expressed by eq. 22a. This may imply that the electric current or voltage makes salt accumulate within a pore. This effect was introduced by $\hat{n}_a$ in the expression for $\hat{n}$ of eq. 15. It is necessary to transform q into the salt concentration $\hat{n}_a$:

$$\hat{n}_a = hq, \tag{26}$$

where the numerical constant h is estimated in the appendix.

4. Application of basic equations to each phenomenon

Since the basic equations introduced in the previous sections are those for a general case, it may be desirable to rewrite these equations in a tractable form for describing each case according to experimental conditions.

4.1. Phase transition under equal salt concentrations

Since neither the pressure difference nor the electric current is imposed on the membrane in usual experiments for the investigation of phase transitions of DOPH molecules [1–3], we here consider the case where Δn_a, ΔP_a and I_a are equal to zero. Furthermore, the amount of DOPH adsorbed is so small that the relaxation may be observed under the usual experimental conditions. Penetration of salt into pores may therefore be much faster than the movements of DOPH molecules in pores, and the salt concentration n_i in pores is expected to equal the external ones n_o in cells.

The following set of equations is sufficient for describing the phase transition of DOPH: kinetic equations given by eq. 8 or 11 with the rate constants, eqs. 9, 10 and 13, where n_t and l are set equal to n_o and L, respectively. The observed electric capacitance can be safely approximated by eq. 19a, which explains fairly well the transition characteristics that relaxation curves are sigmoid after an increase in salt concentration, while the curves are exponential in form after a decrease [3].

4.2. Self-sustained oscillations

4.2.1. Long-period oscillations

Since large amounts of adsorbed DOPH are necessary for the occurrence of oscillation, kinetic changes in n_t can no longer be neglected. As seen later, the membrane potential V is negligibly small. Neglecting V in eq. 5, therefore, length l without ΔP_a is rewritten from eq. 6 as

$$l = \frac{\Delta n_t}{\Delta n_a} L. \tag{27}$$

Taking account of experimental conditions of $n_t = 5$ mM and $\Delta n_a = 95$ mM, l equals $(5/19)L$ for $n_t = 30$ mM.

It may be more convenient to use the simplified eqs. 11a and b in this case. Under the condition of $I_a = 0$, the observed quantity such as the membrane potential is given from eq. 24a as follows:

$$V = -\frac{R}{R + R_0} E_N, \tag{28}$$

where E_N and R are expressed by eqs. 21 and 22b, respectively. While the last term in eq. 15, $\hat{n}_a$, originates from V, as seen from eqs. 25 and 26, it is negligibly small for V of about 100 mV. It implies that the salt accumulation due to V does not affect self-sustained oscillations. We can, therefore, approximate eq. 15 by

$$\hat{n} = X_N[X_A + (1 - X_A)\hat{f}_1(\xi)] \times [1 - (1 - X_B)\hat{f}_2(\eta_m)]. \tag{29}$$

The membrane potential of long-period oscillations can be calculated as follows: eqs. 11a, 11b and 14 with subsidiary eqs. 16 and 29 are solved numerically using the rate and diffusion constants expressed by eqs. 9, 10, 13, 17 and 18 for l given by eq. 27. If the calculated n_t is put into $R(n_i, \tilde{n}_i)$ of eq. 22b with eq. 23, then the membrane potential is described by eq. 28. As can be understood from the above procedure, the kinetic equations for DOPH and n_i do not interact with V directly, because of the omission of $\hat{n}_a$ in eq. 15.

When the electric current I_a is imposed on the membrane showing long-period oscillations, the term $\hat{n}_a$ can no longer be neglected because of

large values of V reaching a few volts. The procedure for calculation in this case is almost the same as that for short-period oscillations under I_a and/or ΔP_a, and hence is detailed below.

4.2.2. Short-period oscillations

Considering first the case in the presence of Δn_a and ΔP_a [5], we can use almost the same equations as for long-period oscillations under $I_a = 0$. While V and $\hat{n}$ are reduced to eqs. 28 and 29, respectively, the length l must be used in the form of eq. 6 with eq. 7. It may be possible to neglect the effect of V on l in this case as well. As can be seen from the expressions for the rate and diffusion constants of eqs. 13 and 18, the frequency of oscillation is expected to increase for decreasing l as increasing ΔP_a shown in eq. 6.

If an electric current is also imposed on the membrane, $\hat{n}_a$ is no longer negligible because the voltage reaches a value as large as a few volts. In other words, the salt accumulation due to the voltage becomes effective on self-oscillations. A procedure in this case is as follows: kinetic equations 11a, 11b and 14 are solved numerically using subsidiary eqs. 15 and 16 with the rate and diffusion constants, eqs. 9, 10, 13, 17 and 18, where $\hat{n}_a$ is given in terms of η_m, n_i, l and I_a by eq. 26 with eqs. 24a and 25 for C and R expressed by eqs. 22a and 22b, respectively. This procedure is performed for ΔP_a and I_a through eqs. 5 and 6 with eq. 24a.

4.2.3. Bursting-like oscillations

Since short-period oscillations are considered to occur in a small proportion of DOPH molecules near the surface due to ΔP_a, the rapid components appearing in bursting-like oscillations also seem to reflect a similar situation casually, since DOPH molecules may also be adsorbed on the surface of filter, as well as in pores. This may be noted if we observe the preparation of the membrane. In fact, DOPH in oil droplets is sometimes visible to the naked eye on the plane surface of a filter when the membrane with large adsorbed amounts is immersed in 5 mM KCl solution.

Fig. 7 illustrates the situation when the burst occurs: the layer of DOPH molecules adsorbed on the surface at the side of lower salt concentration is added to the model shown in fig. 5. This surface layer plays an essential role on the fast component of bursting-like oscillations. It may be reasonable to use the same set of kinetic equations as that for long-period oscillations in discussing the behavior of DOPH adsorbed in a pore. Since DOPH in molecules on the surface may contact n_1 and n_i, however, the expression for $\hat{n}_s$ may be rewritten as

$$\hat{n}_s = Xn_i\left[X_A + (1 - X_A)\hat{f}_1(\zeta_s)\right] \times \left[1 - (1 - X_B)\hat{f}_2(\eta_{ms})\right], \quad (30)$$

where the subscript s denotes the surface, and X is the numerical coefficient. For these molecules, we also use the kinetic equations (eqs. 11a, 11b and 14).

The resistance R may be approximated by

$$R(n_{is}, n_i, \bar{n}_1) = N\left[R_T(n_{is})\frac{l_s}{L} + R_T(n_1)\frac{l}{L} + R_{\bar{T}}(\bar{n}_i)\left(1 - \frac{l}{L}\right)\right], \quad (31)$$

where n_{is} is the salt concentration in the surface region. The length l is equal to $(5/19)L$, the thickness of the surface region l_s possibly being of a much smaller order. Using R, the membrane potential is given by eq. 28.

4.3. I-V characteristics

Let us try to express the situation where the electric current I_a or the electric voltage V_a is imposed on the membrane without Δn_a or ΔP_a as a typical case, since the I-V characteristics are observed irrespective of the presence of Δn_a or ΔP_a. The value of the electric resistance estimated from the jump width of the hysteresis curve shown in fig. 4 suggests that only one to several pores participate in I-V characteristics. We here show a procedure by assuming the number of pores to be unity, which tends to give fairly good agreement with observed data, as will be shown.

Furthermore, we may assume the observed I-V characteristics to reach an almost stationary state because it usually takes several to a few tens of minutes for one scanning of I_a (or V_a), which is much slower than the period of spikes randomly appearing under I_a or V_a [2]. Putting $d/dt = 0$ in eqs. 8a–c and 14 with the salt concentration n_o in

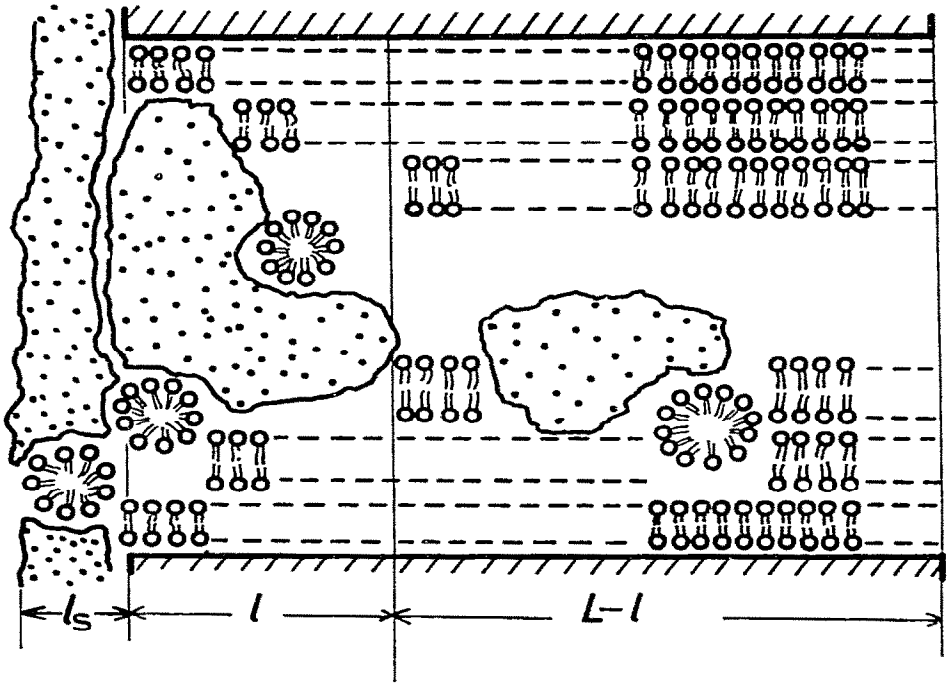

Fig. 7. A model of bursting-like oscillations.

two cells, we obtain

$$\eta_m = \left[1 + \frac{k_{-2}(1+v)}{k_2} + \frac{k_{-1}k_{-2}v}{k_1k_2n_t}\right]^{-1}, \quad (32)$$

$$n_t = \hat{n} = n_0 + \hat{n}_a. \quad (33)$$

Substituting $l = L$ into eqs. 22a and b, we obtain

$$C = \frac{C_T^0}{N}\eta_m, \quad (34a)$$

$$R = NR_-(n_t). \quad (34b)$$

Since the electric capacitance C is expressed as a function of n_t by eqs. 32 and 34a, the relation between V and n_t can be easily obtained from eqs. 25, 26 and 33. As will be shown later, V shows an N-shaped curve for increasing n_t. From eqs. 24a and 34b, therefore, the relation between I and V can be obtained numerically.

5. Comparison with observed data

Fig. 8 shows results calculated for the long-period oscillation. The values of numerical parameters adopted in the present numerical calculations are listed in the figure legend. The wave form is really spike-like and the amplitude is about 30 mV, which are consistent with the observed self-oscillation as shown in fig. 1. It is noticeable that the fraction of multilayer η_m varies with a triangular wave form, which means that the period is determined by the slow change in η_m. The rapid increase in ζ occurs after η_m has decreased. The resultant change in electric resistance is reflected by the rapid change in membrane potential.

In fig. 8b, the relation between the pulse width and period is also shown. To describe theoretically the observed fact that the period increases as the

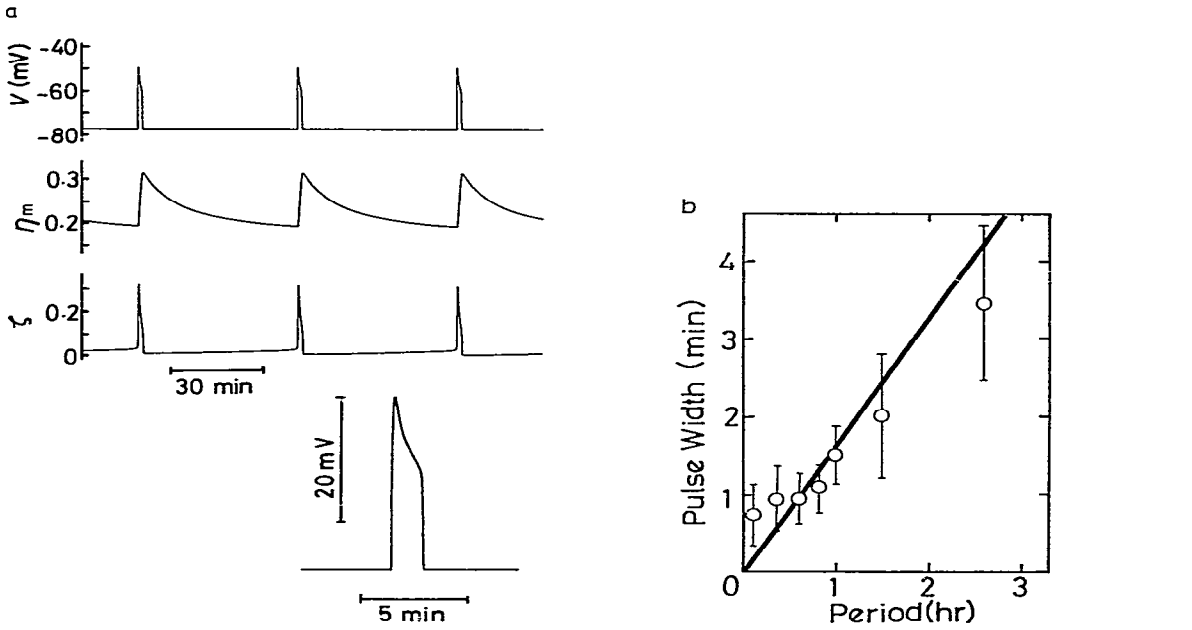

Fig. 8. Theoretical results of long-period oscillations. The numerical parameters were chosen as follows: $k_1^* = 2.63\times10^{-3}$, $k_{-1}^* = 0.526$, $k_2/k_{-2}^0 = 35$, $d_1 = \hat{d}_1 = 4$, $d_2 = \hat{d}_2 = 50$, $v = 100$, $D_0^* = 3.95\times10^{-6}$, $L = 0.01$, $X_N = 324$, $X_A = 0.04$, $X_B = 0.2$, $\gamma = 3.5$, $\gamma' = 3.0$, $\zeta_c = \eta_{mc} = 0.105$, $\hat{D}_0^* = 5.19\times10^{-2}$, $n_1 = 30$, $C_T^0 = 3\times10^5$, $R_0 = 10$, $Nr_1 = 5\times10^6$, $Nr_n^0 = 2500$, $\hat{\gamma} = 0.8$ and $\bar{\eta}_m = 0.7$. (b) D_0^* was changed in proportion to $\hat{D}_0^*$. (○) Experimental data [7] (vertical bars denote the variance); (———) theoretical result. For the effect of I_a on self-oscillations, $L_v/\bar{D}$ was chosen as 1000. See details in the Appendix for the choice of parameter values.

amount of DOPH adsorbed (Q) is increased, the values of D_0^* and $\hat{D}_0^*$ are decreased proportionally, because these quantities may reflect directly the packing density of DOPH within pores. It can be seen that the theoretical result explains fairly well the experimental one [7].

The effect of the imposed current I_a on self-oscillations was investigated theoretically: the period decreases when I_a is imposed, and for I_a above 0.036 μA the oscillation stops. These facts agree qualitatively with the observed data [7].

Fig. 9 shows an example of calculated short-period oscillation and the relation between the frequency and applied pressure difference ΔP_a and/or the electric current I_a. The case of imposed ΔP_a is shown in fig. 9a and b, the case of imposed ΔP_a and I_a being given in fig. 9c. The theoretical results can explain fairly well the occurrence of self-oscillations with a period of about 1 s as well as the observed linear relation between frequency and ΔP_a and also I_a [5,6]: increasing ΔP_a or I_a induces the self-oscillation and furthermore linearly raises the frequency of oscillation. Although the theoretical wave form does not seem to resemble well the observed ones, a marked difference between the spike-like wave form of long-period oscillations and the relatively smooth wave form of short-period oscillations may be expressed fairly well. In addition, the amplitude of oscillation calculated numerically is 16 mV, which shows a good agreement with the observed amplitude of nearly 15 mV [5]. While the amplitude reaches about 200 mV when the electric current is also imposed as shown in fig. 2, the numerical result in the present model with $I_a = 0.3$ μA and $\Delta P_a = 15$ cmH_2O gives an amplitude of about 280 mV in

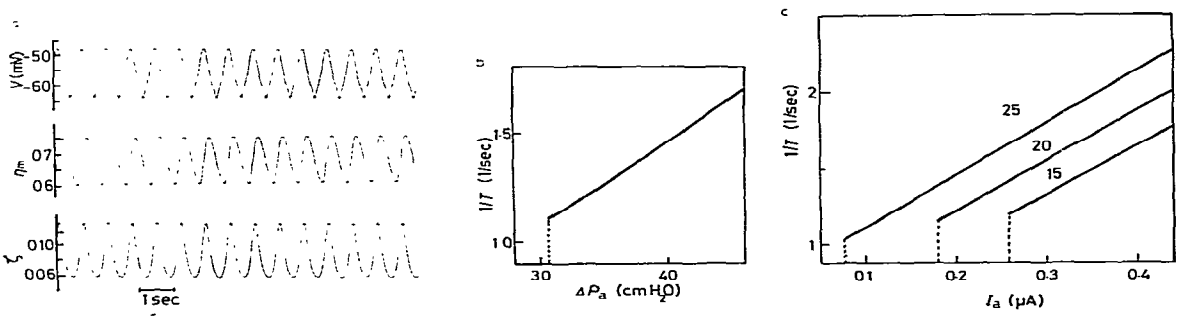

Fig. 9. Theoretical results of short-period oscillations. The numerical parameters are given by $k_2/k^0_{-2} = 10$, $X_A = 0.1$, $X_B = 0.6$, $D_0^* = 10^{-4}$, $\tilde{D}_0^* = 1.23 \times 10^{-3}$, $\bar{\eta}_m = 0.01$ and $L_p/\tilde{D} = 100$. The other parameters have the same values as those in fig. 8. An example of wave forms with $\Delta P_a = 42$ cmH$_2$O and $I_a = 0$ is shown in panel a. The dependence of the frequency $(1/T)$ on ΔP_a with $I_a = 0$ is shown in panel b, and the dependences on I_a with $\Delta P_a = 15$, 20 and 25 cmH$_2$O in panel C.

rather good accord with the observed value. Such a large value arises from the second term in eq. 24a, and is also related to the jump width in the I-V curve.

The occurrence of oscillation can be interpreted as a hard-mode instability. In a similar way to the case of long-period oscillations [7], this type of instability is brought about by the relative increase in the diffusion speed of salt compared with phase-transition speed of DOPH accompanied by increasing ΔP_a or I_a. Since the length l and the number of DOPH molecules involved in oscillations decrease with increasing ΔP_a or I_a, the frequency of oscillation is raised as a result of increasing relevant rate and diffusion constants.

The bifurcation induced by ΔP_a or I_a may be considered as the normal type [15], since a distinct hysteresis could not be found as a result of careful numerical calculations with sufficient execution time. An inverted-type oscillation accompanying the hysteresis has been shown theoretically to appear in the case of long-period oscillations [7], and hence this difference in two kinds of oscillations appears strange. However such a situation may possibly arise because the values of parameters are chosen as somewhat different from each other so that the difference of wave forms can be expressed well. The observed hysteresis [5,6], therefore, could be time-dependent bearing in mind the fast scan rate as usually performed; it belongs to the scan-rate-dependent hysteresis accompanied by a dynamic metastability [3]. Detailed experiments to determine whether the bifurcation is of the normal or inverted type seem nevertheless rather difficult because the bifurcation point is poorly reproducible.

Although the electric current I_a stops the long-period oscillation, I_a induces the short-period

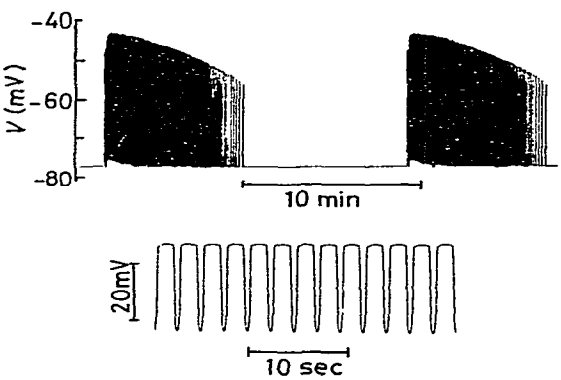

Fig. 10. Theoretical results of bursting-like oscillations. The lower trace is a magnification of part of the wave bundles in the upper trace. Numerical parameters for self-oscillations of DOPH molecules within the pore were chosen as $k_2/k^0_{-2} = 6.5$, $X_A = 0.06$, $X_B = 0.6$, $D_0^* = 1.58 \times 10^{-6}$ and $\tilde{D}_0^* = 2.08 \times 10^{-2}$. The other parameters have the same values as those in long-period oscillations in fig. 8. Parameters for DOPH on the surface are $k_{1s} = 0.13$, $k_{-1s} = 26.3$, $D_{0s} = 5 \times 10^{-3}$, $\tilde{D}_{0s} = 7.0$, $X = 1.5$ and $l_s/L = 0.01$ with the other parameter values being the same as those in the short-period oscillations in fig. 9.

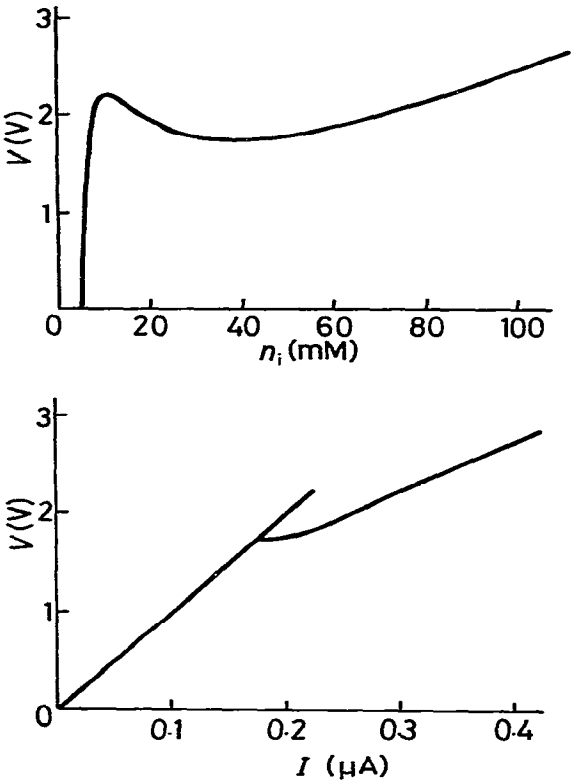

Fig. 11. Theoretical results of I-V characteristics with $\Delta n_a = \Delta P_a = 0$. The values of numerical parameters are those of fig. 9.

oscillation. This apparent contradiction is discussed in detail in the following section.

A calculated example of bursting-like oscillations is shown in fig. 10. It can be seen that the oscillation contains successive bundles composed of oscillations with a period of several seconds, as is the experimental case shown in fig. 3.

Fig. 11 shows an example of calculated results on I-V characteristics. The theoretical I-V curve can be seen to display a hysteresis curve of I with variation in V_a as well as a hysteresis curve of V under control of I_a. This surely agrees with the observed data [2,6]. A hysteretic feature already appears in the relation between V and n_i, and hence it is directly reflected by the I-V relation, as can be seen from eqs. 24a and 34b. The N-shaped curve of V vs. n_i originates from the following process: the voltage V accumulates salt within the pore through the equivalent electric capacitance. This leads to a transformation of DOPH from oil droplets to micelles and multilayers. As a result, the electric capacitance increases, which brings about further salt accumulation. Since it proceeds in a positive feedback way, it now becomes possible for the negative slope of V to appear. The steep and gentle slopes reflect low and high electric capacitances, respectively.

6. Discussion

We now discuss the effect of the imposed current I_a on self-oscillations: I_a stops the long-period oscillation but induces the short-period oscillation. To clarify this apparent contradiction, we must first take into account a difference of the experimental situations between these two types of oscillations. As mentioned in section 2, short-period oscillations are usually observed soon after the membrane is placed between two cells in the presence of ΔP_a and/or I_a, while long-period oscillations appear several hours later with neither ΔP_a nor I_a. In other words, the majority of the DOPH molecules remain in the oil-droplet phase in short-period oscillations but transfer to micelles and multilayers in long-period oscillations, because the phase transition of DOPH from oil droplets to multilayers takes several hours or more to reach completion [3].

This situation is theoretically reflected in the present theory as the value of fraction of multilayers $\bar{\eta}_m$ in the higher salt-concentration region: values of $\bar{\eta}_m$ are chosen as 0.7 and 0.01, as shown in the legends to fig. 8 for long-period oscillations and fig. 9 for short-period ones.

Next, we must note further two competitive effects of the imposed current I_a on oscillations; one is the effect that the presence of I_a tends to shorten the length of the phase-transition region l through electro-osmosis expressed by eqs. 5 and 6 with V related to I_a in eq. 24a. Increasing I_a increases the rate and diffusion constants k_1, D_0,

$\hat{D}_0$ etc., which are explicitly expressed by eqs. 13 and 18. The diffusion speed of salt becomes large at a faster rate than the phase-transition speed of DOPH, as can be seen from the dependences of these kinetic constants on I. As already mentioned, by means of a phase diagram to explain the spontaneous occurrence of long-period oscillations [7], the self-oscillation can be expected to appear through almost the same mechanism. The other effect is that the presence of I_a accelerates the accumulation of salt within the pore, which can be expressed by the relations of eqs. 24a, 25 and 26 through the electric capacitance C of eq. 22a. This effect generally makes it difficult for the self-oscillation to continue, since both release and accumulation of salt are necessary for the occurrence of self-oscillation. A steady accumulation of salt through the capacitance prevents the release of salt from occurring repeatedly and causing the decrease in salt concentration n_t in the phase-transition region.

Taking into account the above-mentioned difference of experimental situations in two kinds of oscillations and also these two contrasting effects of I_a on oscillations, we can understand the effects of I_a on long-period and short-period oscillations in terms of the electric capacitance C. The value of C becomes a few $\mu F/cm^2$ for $\bar{\eta}_m = 0.7$ and several nF/cm^2 for $\bar{\eta}_m = 0.01$. From eqs. 24a, 25 and 26 for expressing the salt accumulation through C in the presence of electric voltage, the steady accumulation of salt cannot be neglected for long-period oscillations but is negligible for short-period oscillations. In fact, the accumulated salt expressed by $\bar{n}_a$ reaches several ten mM with $I_a = 0.1$ μA for long-period oscillations while it stays in negligibly small values as a few mM at most for short-period ones. Although the steady salt accumulation such as several ten mM is sufficient to stop the long-period oscillations, the accumulation of a few mM scarcely affects the short-period oscillations. In other words, the salt accumulation and the relative increase in diffusion speed of salt due to the imposed current play a major role in long- and short-period oscillations, respectively.

This fact leads to the suggestion on the effects of I_a that long-period oscillations are forced to stop by salt accumulation owing to the high electric capacitance, whereas short-period oscillations are induced by the relative increase in diffusion speed of salt accompanied with the decrease in I.

Now let us discuss the difference of wave forms between long- and short-period oscillations as shown in figs. 8 and 9. Such a difference originates mainly from that of the relative magnitude of diffusion speed of salt compared with the phase-transition speed of DOPH. In long-period oscillations, numerous DOPH molecules repeat very slow phase transitions among three phases of oil droplets, spherical micelles and multilayers. The phase-transition speed is therefore much smaller than the diffusion speed of salt. As soon as the overall conformational states of DOPH are able to allow salt to be accumulated or released, the salt concentration within the pore changes rapidly. This rapid change can be observed as rather discontinuous change in the membrane potential represented by spike-like wave forms. Accumulated salt can be released for several minutes during the occurrence of spike.

In short-period oscillations, on the other hand, the phase-transition speed is of comparable order to the diffusion speed of salt because only a tiny proportion of DOPH molecules near the surface of filter are involved in self-oscillations. In this situation, nearly sinusoidal or even distorted but smooth wave forms can be expected to be observed, as shown in figs. 2 and 9.

Whereas some difference is found in the wave form shown in figs. 2 and 9a, it may be partly because the best selection of parameter values in the calculations is not made. We chose the values of some parameters as different from those of long-period oscillations, while most other parameters were selected to be the same (see table 1). Although the present theory can explain well various features of short-period oscillations such as the occurrence with ΔP_a or I_a and the much shorter duration than that of long-period ones, quantitative explanation of the wave forms seems difficult. If we could choose the parameter values so that the observed wave forms could be reproduced satisfactorily, more detailed explanations of the relation between long-period and short-period oscillations might be possible. In practice, other wave forms such as a rectangular one are observed

in short-period oscillations [6], and hence quantitative explanations of these wave forms are left for a future task.

In the present model, the e.m.f. in the pore involved in self-oscillations was considered as the diffusion potential and hence as remaining unchanged during self-oscillations. This approximation resembles somewhat that made in the Hodgkin-Huxley equations with the constant e.m.f. given by the Nernst potential for each ion [16], while this is later improved so as to take account of potassium accumulation in the periaxonal space [17]. At the present stage, however, a detailed derivation of a reliable form of the e.m.f. seems to be difficult in the relevant pore, which is occupied by numerous charged DOPH molecules repeating conformational changes among oil droplets, micelles and multilayers.

Finally, let us discuss self-sustained oscillations which probably result from two pores as shown in fig. 12. This type of oscillation has sometimes been observed. However, each period of self-oscillation resulting from the different pore is not always constant, and in many cases oscillations finally decline after several hours. This fact suggests that these two self-oscillations do not occur quite independently. In fact, an example of synchronized oscillations is also reported in short-period oscillations [18]. Although a detailed mechanism of interaction between two oscillations appearing at the same time cannot be explained precisely as yet, it does seem to be related to the condition in the pore concerned: all the pores are not divided proportionally but a part of them branches. A pore at one side of a Millipore filter may often branch off into two pores at the other. If the oscillation occurs by chance in such a branched pore regarded as two pores in the phase-transition region, it can produce two oscillations with different or the same periods according to various conditions, e.g., overall conformational states of DOPH and the shape of the pore because the direct interaction can be expected through the mutual change in the salt concentration within the pores. Even when two oscillations occur in two pores separated spatially, there may exist very weak interactions such as the conformational change in DOPH adsorbed on the filter surface due to the change in salt concentration near the surface accompanied by the oscillation for the membrane with the larger amount of DOPH adsorbed. If the solitary oscillation starts casually in a distinct single pore with no branch, on the other hand, it may continue independently owing to little interference from and on other pores. It seems to be dominated by the preconditions of DOPH adsorbed in the filter if one, two or more oscillations appear in separate or branched pores. Further discussions of these points may be left as an interesting problem.

Acknowledgements

The numerical calculations in the present work were performed with the aid of FACOM M-200 in Kyushu University Computer Center. This work was supported in part by a Grant-in-Aid (No. 58780253) for the Encouragement of Scientists.

Appendix

In the present theory, the values of numerical parameters for kinetics of DOPH molecules are determined from kinetic experiments [3]. However, for D_0^*, much smaller values are adopted because the amounts of DOPH adsorbed are larger in the experiments for self-oscillations than those for kinetics of the phase transition. Explicit values of parameters are summarized in table 1 where two values are shown for each parameter (D_0^*, k_2/k_{-2}^0, $\hat{D}_0^*$, X_A, X_B and $\bar{\eta}_m$) with the values on the left and right corresponding to long-period oscillations (period 51.7 min) and short-period ones, respectively.

Almost all the numerical parameters for kinetics of salt are taken from the previous paper on self-oscillations [7]. The diffusion constant $\hat{D}$ of salt within the pore can be estimated from the values of $\hat{D}_0^*$ listed in table 1 and eqs. 17 and 18: using the value for long-period oscillations, it leads to about 10^{-7} cm^2/s within the pore mainly occupied by oil-droplet phases and several 10^{-6} cm^2/s for multilayer phases. Taking into account the fact that the diffusion constant of K^+ in the

Table 1

Values of numerical parameters adopted in the theoretical description

Kinetics of DOPH molecules		Kinetics of salt		Electric characteristics	
$\mathcal{D}_0^*$	3.95×10^{-6}–10^{-4} (s^{-1})	$\tilde{D}_0^*$	5.19×10^{-2}–1.23×10^{-3} (s^{-1})	C_0	10^{-4} (pF)
d_1	4			C_c	10^{2} (pF at 1 kHz)
d_2	50	$\tilde{d}_1$	4	C_T^0	3×10^{5} (pF/cm^2)
k_1^*	2.63×10^{-3} (s^{-1})	$\tilde{d}_2$	50	h	1.74×10^{14} (mM/C)
k_{-1}^*	0.526 (s^{-1})	L	0.01 (cm)	Nr_1	5×10^{6} (MΩ)
k_2/k_{-2}^0	35–10	$L_p/\tilde{D}$	100 (1/cmH$_2$O cm)	Nr_h^0	2500 (MΩ mM)
n_t	30 (mM)	$L_v/\tilde{D}$	1000 (1/V cm)	R_0	10 (MΩ)
c	100	n_h	100 (mM)	R_e	200 (Ω in 50 mM KCl)
		n_1	5 (mM)	$\tilde{\gamma}$	0.8 (mM^{-1})
		X_N	324 (mM)	$\tilde{\eta}_m$	0.7–0.01
		X_A	0.04–0.1		
		X_B	0.2–0.6		
		γ	3.5		
		γ'	3.0		
		ζ_c, η_{mc}	0.105		

aqueous solution is of the order of 10^{-5} cm^2/s. these values within the pore may be considered as fairly reasonable. The value of L_p may lie between 10^{-2} and 10^{-9} in units of cm/s per cmH$_2$O if we use values of 10^{-2} for a membrane filter and 10^{-7}–10^{-9} for biological membranes [19]. Since the equivalent diffusion constant $\tilde{D}$ given by eq. 4 may be taken to be about 10^{-6} cm^2/s from the above discussion of the diffusion constant of salt, $L_p/\tilde{D}$ is expected to be 10^{-3}–10^{-4}. We here choose $L_p/\tilde{D}$ to be 10^{2} in order to express quantitatively the observed threshold value of ΔP_a. The value of $L_v/\tilde{D}$ is also chosen to express well the observed threshold I_a.

Such quantities as the electric capacitance and resistance contained in the equivalent electric circuit are also summarized in table 1. The electric quantities C_0 and R_0 resulting from almost all pores, where DOPH molecules do not participate in self-oscillations, are considered as those at lower salt concentrations due to very slow phase-transition speed and little penetration of salt. In fact, the electric resistance amounts to several megaohms or more even under the salt difference Δn_a, if adsorbed DOPH amounts are large, which is the case in these kinds of experiments. The quantities C_0 and R_0 are therefore taken to be 10^{-4} pF and 10 MΩ as typical values. The maximum electric capacitance per unit area C_T^0 is chosen as 3×10^{5} pF/cm^2 by adopting values obtained at higher salt concentrations.

Let us next estimate the value of h, which is the factor for translating the accumulated charge q in the condensor to the accumulated salt concentration $\hat{n}_a$. By applying the electric current I_a or voltage V_a on the membrane, an electric double layer is expected to form within the pore almost parallel to the filter surface. If salt is assumed as accumulating uniformly in the region with Debye length, λ_D, as a rough approximation, the salt concentration $\hat{n}_a$ can be given by

$$\hat{n}_a = Nq/\lambda_D. \tag{A1}$$

The Debye length λ_D is about 10 Å for 100 mM salt concentration. We choose a smaller value, 6 Å, as λ_D by taking account of the high electric voltage difference of a few volts induced by the electric current of the order of 0.1 μA, for example. Putting this value into eq. A1, we obtain 1.74×10^{14} mM/C as h.

The electric resistance R given by eq. 22b is mainly composed of two resistances. One is Nr_1 at lower salt concentrations, the other being Nr_h^0/n_i at higher salt concentrations. The value of Nr_1 is chosen to be 5×10^{6} MΩ, since it may correspond to NR_0 with N equal to about 10^{6} cm^{-2}. The resistance Nr_h^0/n_i can be written in terms of an equivalent conductivity of the electrolyte solution,

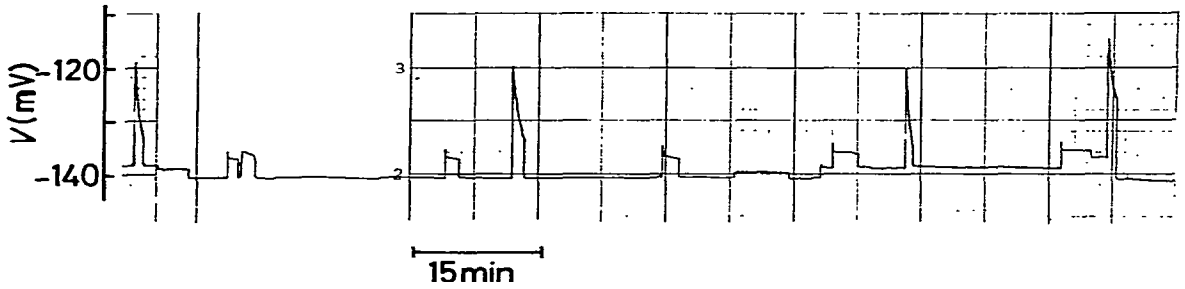

Fig. 12. An example of oscillations resulting from two pores.

λ, the thickness of filter L and the sectional area a as follows:

$$Nr_h^0/n_i = 10^6 \times L/\lambda a n_i. \quad \text{(A2)}$$

Since λ is about 150 cm^2/Ω per equiv. for KCl and L is equal to about 0.01 cm, eq. A2 leads to

$$Nr_h^0/n_i = 3700/an_i. \quad \text{(A3)}$$

If we assume that a circular area of radius 1 μm becomes open, Nr_h^0 gives a value of about 2500 in the units of MΩ mM. As shown in the theoretical result depicted in figs. 8, 9 and 11, the pulse height and amplitude of self-oscillations as well as the change in voltage or current in I-V characteristics agree fairly well with the observed data. This means that only one pore is involved in self-oscillations, as suggested previously [6,7].

However, oscillations resulting from probably two or more pores are also sometimes observed. An example is shown in fig. 12, where two sorts of oscillations with explicitly different pulse heights appear at the same time. This type of oscillation does not continue stably for more than several hours, while self-oscillations resulting from one pore usually continue for a day.

References

1 Y. Kobatake, A. Irimagiri and N. Matsumoto, Biophys. J. 10 (1970) 728.
2 Y. Kobatake, Adv. Chem. Phys. 29 (1975) 319.
3 K. Toko, J. Nitta and K. Yamafuji, J. Phys. Soc. Jap. 50 (1981) 1343.
4 N. Kamo, T. Yoshioka, M. Yoshida and T. Sugita, J. Membrane Biol. 12 (1973) 193.
5 J. Arisawa and T. Furukawa, J. Membrane Sci. 2 (1977) 303.
6 K. Urahama and K. Yamafuji, Trans. IECE Japan 65C (1982) 185 (in Japanese).
7 K. Toko, K. Ryu, S. Ezaki and K. Yamafuji, J. Phys. Soc. Jap. 51 (1982) 3398.
8 S. Tokutomi, G. Eguchi and S. Ohnishi, Biochim. Biophys. Acta 552 (1978) 78.
9 I. Prigogine and R. Lefever, Adv. Chem. Phys. 39 (1978) 1.
10 Y. Kobatake and H. Fujita, J. Chem. Phys. 40 (1964) 2212.
11 M.H. Cohen and D. Turnbull, J. Chem. Phys. 31 (1954) 1164.
12 H. Träuble, M. Teubner, P. Woolley and H. Eibl, Biophys. Chem. 4 (1976) 319.
13 K. Toko and K. Yamafuji, Biophys. Chem. 14 (1981) 11.
14 J. Heicklen, Colloid formation and growth (Academic Press, New York, 1976).
15 Y. Kuramoto and T. Tsuzuki, Prog. Theor. Phys. 54 (1975) 687.
16 A.L. Hodgkin and A.F. Huxley, J. Physiol. 117 (1952) 500.
17 W.J. Adelman, Jr and R. FitzHugh, Fed. Proc. 34 (1975) 1322.
18 K. Urahama, Trans. IECE Japan 64C (1981) 453 (in Japanese).
19 A. Katchalsky and P.F. Curran, Nonequilibrium thermodynamics in biophysics (Harvard University Press, Cambridge, MA, 1965).